CrystEngComm

Accepted Manuscript

ROYAL SOCIETY OF CHEMISTRY

www.rsc.org/crystengcomm

Journal Name

RSCPublishing

ARTICLE

Cite this: DOI: 10.1039/x0xx00000x

Received xxxxxxxxx
Accepted xxxxxxxxx

DOI: 10.1039/x0xx00000x

www.rsc.org/

Tuning the formation of dicarboxylate linker-assisted supramolecular 1D chains and squares of Ni(II) using coordination and hydrogen bonds†

Sadhika Khullar[a], Vijay Gupta[a] and Sanjay K. Mandal[a]*

Based on the variation in the multitopic dicarboxylates differing in the aliphatic chain structure (triple bond to double bond to single bond, respectively) in the formation of diverse coordination architectures for the same metal center and the ancillary ligand bpta, three new metal organic coordination networks (MOCNs) $[Ni(bpta)(adc)(H_2O)_2]\cdot 2H_2O$ (**2**), $[Ni_4(bpta)_4(fumarate)_4(H_2O)_4]\cdot 4H_2O$ (**3**) and $[Ni(bpta)(succinate)(H_2O)_2]\cdot 3H_2O$ (**4**) are reported here (where bpta = N,N′-bis(2-pyridylmethyl)-tert-butylamine and adc = acetylene dicarboxylate). These are synthesized in good yields from a one-pot self-assembly reaction using $Ni(OAc)_2$, bpta and the corresponding acid in methanol at ambient conditions. In order to shed light into their formation, the intermediate compound $[Ni(bpta)(OAc)_2(H_2O)]\cdot H_2O$ (**1**) from the two-component mixture ($Ni(OAc)_2$ and bpta), for all MOCNs has also been isolated and crystallographically characterized. Through strong hydrogen bonding between coordinated water, uncoordinated oxygen atoms of the two acetate groups and the lattice water molecule, **1** has a 1D chain structure. In **2** and **4**, only one end of the dicarboxylate is coordinated to Ni(II) due to the fact that its other end (a carboxylate group *not* a carboxylic acid group which is commonly found for numerous polycarboxylic acids under hydrothermal conditions) is strongly hydrogen bonded to two coordinated water molecules of the adjacent Ni(II) center of the monomeric unit generating a 1D chain which is further hydrogen bonded through the lattice water molecules to form the respective 2D supramolecular assemblies. On the other hand, bis(monodentate) syn-syn and syn-anti bridging modes of fumarates between two Ni(II) centers result in the formation of a square in **3**. These squares in **3** are further associated via hydrogen bonding through the formation of a six membered hexagonal motif $R_4^6(6)$ between two lattice water molecules, uncoordinated oxygen atoms of the fumarate and two coordinated water molecules on Ni(II) centers. The strength of hydrogen bonding observed in the networks of **2**-**4** (the range of O---O distances is 2.638 Å to 2.949 Å) are very similar to those found in water and ice. All these are characterized by elemental analysis, single crystal X-ray diffraction, IR and Raman spectroscopy. Their thermal behavior in the solid state analyzed by thermogravimetric analysis (TGA) shows unusual stability of **3** up to 300 °C compared to **2** and **4**.

Introduction

In the last few decades there has been a growing interest in the synthesis and structural characterization of metal organic coordination networks (MOCNs) for studies in a variety of potential applications, such as catalysis, separation, sensors, gas storage, luminescent materials, ion exchange, magnetism, etc.[1-3] These networks comprised of metal centres and multitopic organic linkers are held together through various interactions, such as metal-donor atom coordinate bonds, strong and/or weak hydrogen bonds, π-π stacking of aromatic moieties, C-H…O interactions, etc.[4] Utilization of the diverse binding modes of carboxylate linkers[5] for the synthesis of such MOCNs requires the proper choice of the ancillary ligand attached to the metal center(s). The use of metal centers or metal atom clusters as the building blocks gives advantages due to different binding abilities of the metal center. The selection of ancillary ligands and the multitopic organic linkers is crucial in making such assemblies with varied dimensionality. The role of ancillary ligands that surround and protect the metal cores leaving open sites for the linkers is of great importance in making such metal

organic coordination networks. In most cases, the hydrothermal/solvothermal method has been employed to synthesize these materials.[6] Use of such method has some limitations, such as poor stability of some carboxylate linkers (e.g., acetylene dicarboxylate (adc)) at high temperature and reproducibility. Therefore, making MOCNs under ambient conditions is an attractive route for its simplicity as well as generalization for similar systems. For our interests to explore and identify the factors governing the formation of supramolecular assemblies vs discrete polygons, such as squares and rectangles, and their further association through supramolecular interactions, a systematic study has been carried using multidentate polypyridyl ancillary ligands and multitopic carboxylate linkers with Ni(II) as the metal center.

In this article, using the tridentate ligand, bpta = N,N′-bis(2-pyridylmethyl)-tert-butylamine we report diverse metal organic coordination networks generated under the same reaction conditions: the fumarate analogue $[Ni_4(bpta)_4(fumarate)_4(H_2O)_4]\cdot 4H_2O$ (**3**) is a square while the adc and succinate analogs $[Ni(bpta)(adc)(H_2O)_2]\cdot 2H_2O$ (**2**) and $[Ni(bpta)(succinate)(H_2O)_2]\cdot 3H_2O$ (**4**) form zigzag and linear 1D chains, respectively; further association of these through extensive hydrogen bonding network of lattice water, coordinated water and uncoordinated oxygen atoms of the carboxylate groups generate supramolecular assemblies of higher dimensions. Also reported is the intermediate prior to the formation of **2-4** upon addition of the respective dicarboxylic acid, $[Ni(bpta)(OAc)_2(H_2O)]\cdot H_2O$ (**1**), which has a 1D chain structure through strong hydrogen bonding between coordinated water, uncoordinated oxygen atoms of the two acetate groups and the lattice water molecule. Scheme 1 shows the structure of the ligand and dicarboxylate linkers used in this study.

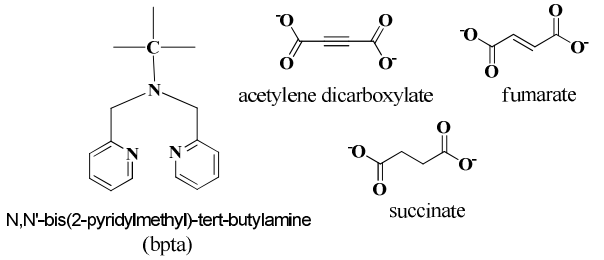

Scheme 1 Structure of the bpta ligand and dicarboxylate linkers used in this study.

Results and discussion

Synthesis. Compounds **2-4** were prepared and isolated from the one pot self-assembly of the metal salt, ligand and dicarboxylic acid (1:1:1 ratio) in methanol under ambient conditions (see Scheme 2). Acetic acid that was the by-product in all reactions was removed completely with a mixture of toluene:acetonitrile (1:1) added to the reaction mixture. Compounds **2** and **4** did not give a precipitate in methanol. On the other hand, compound **3** yielded a precipitate in methanol and thus was re-dissolved in water to grow its crystals; the solid isolated from the reaction is exactly the same as the crystals obtained based on the FTIR spectroscopy data.

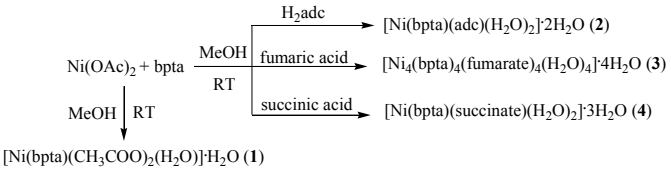

Scheme 1. Synthesis of **1-4**.

Description of Structures. Crystals suitable for the single crystal X-ray study were grown from the cooling of methanolic solution of **2** and slow evaporation of aqueous solution of **3** and methanolic solution of **1** and **4**.

$[Ni(bpta)(CH_3COO)_2(H_2O)]\cdot H_2O$ (1). It is a mononuclear Ni(II) compound that crystallizes in *P-1*. The geometry around Ni(II) center is octahedron surrounded by three nitrogens of the ligand, one coordinated water molecule and two acetates which bind in monodentate fashion as shown in Fig 1. A labelled Fig. S1 is included in the ESI. This is one of the few examples of mononuclear hexacoordinated Ni(II) complexes with one or two monodendate carboxylates.[7-8] The selected bond distances and angles are listed in Table S1 of the ESI. The coordinated water molecule on Ni(II) center shows bifurcated hydrogen bonding; it is strongly and intramolecularly hydrogen bonded (O5…O2, 2.595 Å and O5…O4, 2.696 Å) to the uncoordinated oxygen atom of acetate forming two 5-membered rings ($R_1^1(5)$). In addition to this, lattice water molecule O6 is also hydrogen bonded to O4 (uncoordinated oxygen atom of acetate) forming a 1D chain structure (see Fig 2). All hydrogen bonding parameters are listed in Table 2.

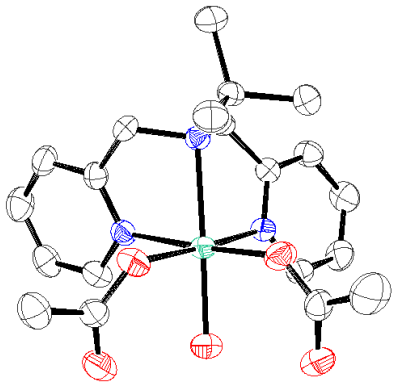

Fig. 1 An ORTEP view of **1**.

$[Ni(bpta)(adc)(H_2O)_2]\cdot 2H_2O$ (2). It crystallizes in the orthorhombic *Pbca* space group. The coordination environment around the Ni(II) center is N_3O_3, where the ligand 'bpta' wraps around the Ni(II) center leaving three open sites for two water molecules and one monodentate adc. An ORTEP drawing of **2** is shown in Fig. 3; a labelled version is shown in Fig. S2, ESI.

Table 1. Crystal Structure Data and Refinement Parameters for **1**, **2**, **3** and **4**.

	1	**2**	**3**	**4**
Chemical formula	$C_{20}H_{31}N_3NiO_6$	$C_{20}H_{29}N_3NiO_8$	$C_{82}H_{108}N_{12}Ni_4O_{24}$	$C_{20}H_{35}N_3NiO_9$
Formula Weight	468.19	498.17	1856.62	520.22
Temperature (K)	270(2)	140(2)	150(2)	150(2)
Wavelength(Å)	0.71073	0.71073	0.71073	0.71073
Crystal system	Triclinic	Orthorhombic	Triclinic	Orthorhombic
Space group	*P-1*	*Pbca*	*P-1*	$Pca2_1$
a (Å)	8.362(2)	13.9083(6)	9.1705(9)	14.5930(13)
b (Å)	9.211(3)	17.7966(7)	14.6580(12)	9.6778(7)
c (Å)	14.892(4)	18.4094(8)	16.5447(16)	17.2357(15)
α (°)	100.999(19)	90	75.264(5)	90
β (°)	94.355(17)	90	83.445(6)	90
γ (°)	97.503(17)	90	87.664(6)	90
Z	2	8	1	4
Volume ($Å^3$)	1110.3(5)	4556.7(3)	2136.6(3)	2434.2(4)
Density (g/cm^3)	0.914	1.452	1.443	1.420
μ (mm^{-1})	0.914	0.902	0.945	0.85
Theta range	1.40 to 25.09°	2.16 to 25.06°	1.28 to 25.14°	2.10 to 25.07°
F(000)	496	2096	976	1104
Reflections Collected	13454	24675	16303	16582
Independent reflections	3893	4028	7539	4267
Reflections with I >2σ(I)	2960	2939	4333	3633
R_{int}	0.053	0.0608	0.0428	0.0552
Number of parameters	285	316	549	314
GOF on F^2	0.974	1.013	0.897	0.968
Final R_1[a]/wR_2[b] (I > 2σ(I))	0.0400/0.0933	0.0374/0.0650	0.0452/ 0.0863	0.0354/ 0.0684
Weighted R_1[a]/wR_2[b] (all data)	0.0601/0.1032	0.0777/0.0880	0.0955/0.1123	0.0467/0.0734
Flack parameter	----------	----------	----------	0.0(0)
Largest diff. peak and hole ($eÅ^{-3}$)	0.318 and -0.386	0.366 and -0.322	0.971 and -0.442	0.187 and -0.307

[a]$R_1 = \Sigma||Fo| - |Fc||/\Sigma|Fo|$. [b]$wR_2 = [\Sigma w(Fo^2 - Fc^2)^2/\Sigma w(Fo^2)^2]^{1/2}$, where $w = 1/[\sigma^2(Fo^2) + (aP)^2 + bP]$, $P = (Fo^2 + 2Fc^2)/3$.

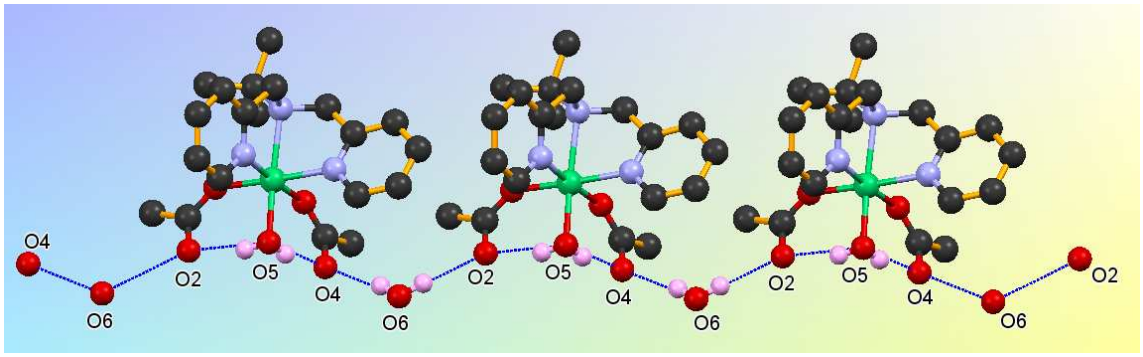

Fig. 2 Schematic representation of the supramolecular assembly in **1** via strong intra- and intermolecular hydrogen bonding interactions.

Table 2. Hydrogen bonding parameters for **1**, **2**, **3** and **4**.[a]

D–H...A	r (D-H) (Å)	r (H…A) (Å)	r (D…A) (Å)	∠D-H…A (deg)	Symmetry
1					
O(5) —H(5A)...O(4)	0.83	1.79	2.595(4)	166	
O(5) —H(5B)...O(2)	0.83	1.89	2.696(4)	164	
O(6) —H(6A)...O(2)	0.85	2.17	3.014(5)	177	1-x,-y,1-z
O(6) —H(6B)...O(4)	0.85	2.11	2.943(5)	167	1-x,1-y,1-z
C(13) —H(13C)...O(1)	0.96	2.36	3.184(4)	144	
C(14) —H(14A)...O(1)	0.96	2.39	3.210(4)	143	
2					
O(1) —H(1A)...O(6)	0.86(3)	1.90(3)	2.751(3)	173(3)	x, 1/2-y, -½+z
O(1)—H(1B)…O(4)	0.82(3)	1.86(3)	2.656(3)	164(3)	
O(2) —H(2A)...O(5)	0.88(3)	1.94(3)	2.794(3)	164(3)	x, 1/2-y, -½+z
O(2)—H(2B)…O(7)	0.82(3)	1.93(3)	2.736(3)	169(3)	1/2+x,y,1/2-z
O(7) —H(7A)...O(8)	0.91(4)	1.98(4)	2.839(4)	175(2)	-1/2+x,1/2-y,-z
O(7)—H(7B)…O(6)	0.82(4)	2.09(4)	2.887(3)	166(3)	x, 1/2-y, -½+z
O(8) —H(8A)...O(5)	0.77(4)	2.15(4)	2.921(3)	174(4)	x, 1/2-y, -½+z
O(8) —H(8B)...O(4)	0.86(4)	1.96(4)	2.819(3)	175(4)	½+x,y,1/2-z
C(3) —H(3A)...O(7)	0.93	2.58	3.367(4)	143	½-x,-1/2+y,z
C(6) —H(6A)...O(5)	0.93	2.36	3.250(3)	159	x, 1/2-y, -½+z
C(14) —H(14C)...O(2)	0.96	2.60	3.428(4)	145	
C(16)—H(16A)…O(2)	0.96	2.52	3.358(4)	146	
3					
O(3) —H(3A)...O(8)	0.85	1.88	2.638(4)	146	
O(3) —H(3B)...O(5)	0.85	1.75	2.538(4)	153	1-x,1-y,1-z
O(7) —H(7A)...O(11)	0.85	1.85	2.622(4)	149	
O(7) —H(7B)...O(10)	0.85	1.84	2.589(4)	145	
O(12) —H(12C)...O(11)	0.85	2.19	3.021(6)	166	
O(12) —H(12D)...O(13)	0.85	2.11	2.949(5)	168	
O(13) —H(13C)...O(3)	0.85	2.00	2.848(4)	177	
O(13) —H(13D)...O(8)	0.85	1.96	2.808(4)	175	1-x,1-y,1-z
C(13) —H(13)...O(13)	0.95	2.32	3.267(6)	177	-x,1-y,1-z
C(15) —H(15A)...O(4)	0.98	2.38	3.231(5)	145	1-x,1-y,1-z
C(16) —H(16C)...O(4)	0.98	2.42	3.270(5)	144	1-x,1-y,1-z
C(18) —H(18)...O(11)	0.95	2.4	3.294(6)	157	x,1+y,z
C(28) —H(28)...O(10)	0.95	2.47	3.226(6)	136	-1+x,y,z
C(35) —H(35C)...O(1)	0.98	2.54	3.261(6)	130	
C(36) —H(36A)...O(6)	0.98	2.33	3.217(6)	150	
C(40) —H(40)...O(12)	0.95	2.59	3.385(6)	142	-x,-y,1-z
C(42) —H(42)...O(13)	0.95	2.55	3.353(6)	142	-1+x,y,z
4					
O(1)—H(1A)....O(5)	0.88	1.80	2.6713	171	x,-1+y,z
O(1)—H(1B)…O(8)	0.80	1.91	2.6858	165	
O(2)—H(2A)...O(6)	0.95	1.82	2.7318	160	x,-1+y,z
O(2)—H(2B)...O(4)	0.95	1.68	2.6083	164	
O(7)—H(7A)…O(5)	0.85	1.92	2.7677	173	-1/2+x,1-y,z
O(7)—H(7B)...O(4)	0.85	2.29	3.0863	157	
O(8)—H(8A)…O(9)	0.85	1.93	2.7596	163	½+x,1-y,z
O(8) —H(8B)…O(2)	0.85	2.14	2.9606	163	½+x,-y,z
O(9)—H(9A)…O(6)	0.85	1.93	2.7684	166	
O(9)—H(9B)…O(7)	0.85	2.03	2.7596	143	
C(8)—H(19)...O(3)	0.98	2.43	3.0845	145	
C(7)—H(24)...O(3)	0.98	2.44	3.2815	145	

[a]Numbers in parenthesis are estimated standard deviations in the last significant digits.

Journal Name RSCPublishing

ARTICLE

The selected bond distances and angles around Ni(II) center are listed in Table S1 of the Supporting Information. The bond distances are similar to those found in other nickel(II)-bpta complexes, particularly the mononuclear complex $[Ni(bpta)(H_2O)_3](ClO_4)_2$.[9] Recently, we have shown the importance of the coordinated water molecule on each Mn(II) center which provided the hydrogen bonding for the formation of a 2D supramolecular assembly of $[Mn_2(adc)_2(bpta)_2(H_2O)_2]$ (adc = acetylene dicarboxylate) while its hydrated species, $[Mn_2(adc)_2(bpta)_2(H_2O)_2]\cdot 6H_2O$, has further connection of the 2D network with the cluster of six water molecules via strong hydrogen bonding interactions forming the 3D supramolecular assembly.[10] Therefore, for the chemistry of Ni(II) under identical reaction conditions it is expected to have the product with the same structure found in case of Mn(II) as both metal centers prefer to have hexa-coordination but Ni(II) provides a different product. Although a dicarboxylate is used, only one carboxylate group binds in a monodentate mode to the Ni(II) center allowing water molecules to coordinate to the Ni(II) center. The reason for the other end of the dicarboxylate not binding to another Ni(II) center in **2** is the strong hydrogen bonding between carboxylate group and two coordinated water molecules on Ni(II). This results in the formation of a 1D zigzag chain of **2** as shown in Fig 4 (top). It is one of the rarest examples where only one end of a dicarboxylate binds to a metal center.[11] Lang et al. has reported a similar binding mode of ferrocene dicarboxylate (fcdc) in $[Cu(pmdta)(fcdc)(H_2O)]\cdot CH_3OH$,[11] where pmdta is pentamethyldiethylenetriamine, which also forms a 1D chain structure through the hydrogen bonding between the coordinated water molecule and one of the oxygens of the uncoordinated carboxylate group of fcdc. However, this chain structure differs from that observed in **2** due to the presence of two coordinated water molecules both of which are involved in hydrogen bonding with both oxygens of the uncoordinated carboxylate of adc. The O--H...O distances between the coordinated water molecules (O1 and O2) and the oxygen atoms (O6 and O5) of the free end of carboxylate are 2.751 Å and 2.794 Å, respectively, which are close to those found in discrete water clusters or encapsulated water clusters in MOCNs.[12-13] Further hydrogen bonding of two lattice water molecules with coordinated water molecules and uncoordinated oxygen atoms of adc makes it a 2D supramolecular assembly (Fig 4, bottom). This is responsible for the formation of three motifs - one heptagon $R_4^7(7)$ labeled as 1, one octagon $R_2^4(8)$ labeled as 2 and one decagon $R_3^4(10)$ labeled as 3 in Figure 2. Motif 1 composed of O2…O5…O8…O4…O1…O6…O7, Motif 2 has O5…O8…O7…O2…Ni…O3 and 4 carbons of adc and Motif 3 has O8…O7…O6…carbon atoms of adc…O4. **2** is an example of a monomeric synthon forming a supramolecular assembly. It should be noted here that further association of the 1D chain of **2** due to the presence of lattice water molecules is absent in the Cu(II)-fcdc compound mentioned above. All hydrogen bonding parameters are listed in Table 2. Further, this supramolecular assembly is also stabilized by several C--H…O interactions listed in Table 2.

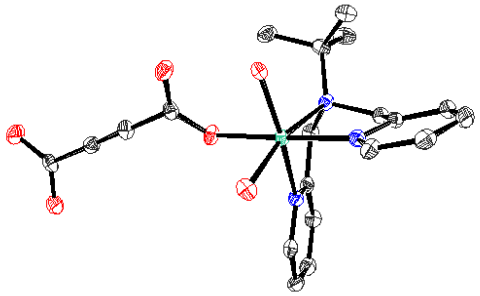

Fig. 3 An ORTEP view of **2**.

$[Ni_4(bpta)_4(fumarate)_4(H_2O)_4]\cdot 4H_2O$ (3). It crystallizes in the triclinic *P-1* space group. Unlike the adc (*vide supra*) and succinate (*vide infra*) analogs, the fumarate analogue is structurally different. It is a square with sides made up of bridging fumarates; in the asymmetric unit in addition to one molecules of the square that sits on an inversion center, there are four lattice waters. The pore size of the square is 12.805 Å x 13.693 Å (Fig 5). Each hexacoordinated Ni(II) center is surrounded by one bpta ligand, one water molecule and two oxygens from two fumarates that binds in a bis(monodentate) syn-syn as well as syn-anti fashions (see Fig S3, ESI). The geometry around Ni(II) centers is distorted octahedron. The selected bond distances and angles are listed in Table S1 of the ESI. The orientation of coordinated water moleucles on Ni(II) centers are different - two are pointing inside the cavity while the other two are pointing outside the cavity. Only a few tetranuclear Ni(II) squares are reported in the literature: one with a tetradentate carboxylate-appended pyridyl ligand where each Ni(II) center is pentacoordinated[14] and the others with nitrogen based ligands where each Ni(II) center is hexacoordinated similar to **3**.[15] To the best of our knowledge, with the combination of polypyridyl ancillary ligand and dicarboxylate this is the first example of a square containing Ni(II).

These squares in **3** are further associated via hydrogen bonding between two lattice water molecules, uncoordinated oxygen atoms of the fumarate and two coordinated water molecules on Ni(II) centers (on opposite corner of the square) forming a six membered hexagonal motif $R_4^6(6)$ labeled as 1 (O3…O13…O8…O3′…O13′…O8′; distances: 2.848(4), 2.808(4) and 2.638(4) Å) in Fig 6. Other two lattice water molecules (O12 and O13) molecules are positioned as dangling

Journal Name RSCPublishing

ARTICLE

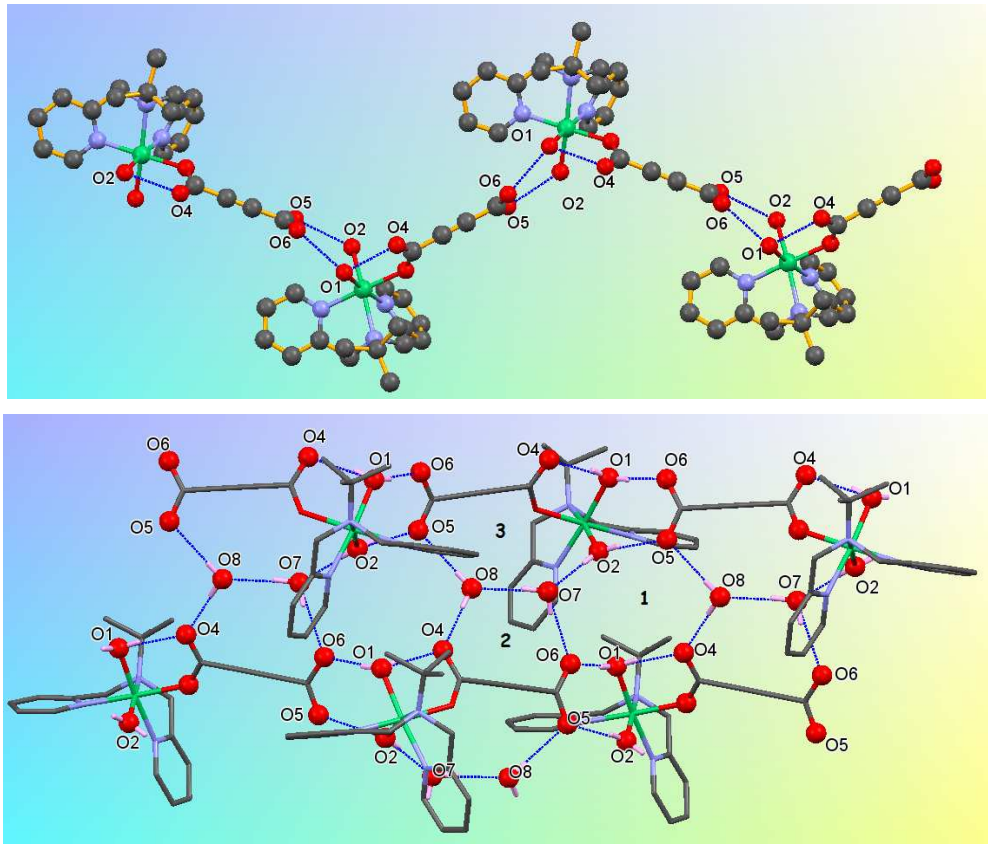

Fig. 4 1D zigzag chain of **2** (top) and formation of a 2D supramolecular assembly from the 1D chains and lattice water molecules in **2** (bottom).

monomers through hydrogen bonding (distances: 2.949(5) Å) on each side - perpendicular to the propagation of the squares in the supramolecular assembly - of the hexagonal motif. On each corner of the square, the coordinated water molecule show strong intramolecular hydrogen bonding to the uncoordinated oxygen atoms of the carboxylate group, e.g., O7 is intramolecularly hydrogen bonded to O10 and O11 (distances: 2.589(4) and 2.622(5) Å). Further, this supramolecular assembly is also stabilized by C-H…O interactions listed along with other hydrogen bonding interactions in Table 2.

[Ni(bpta)(succinate)(H_2O)$_2$]·3H_2O (4). It crystallizes in the monoclinic *P*ca2$_1$ chiral space group. The coordination environment around Ni(II) is similar to that in **2** (see Fig. 7) but the hydrogen bonding interactions are different. A labelled Fig. S4 is included in the ESI. The selected bond distances and angles are listed in Table S1 of the ESI.

Like in **2**, only one end of the succinate binds to the Ni(II) center of **4** in a monodentate fashion and other end is strongly hydrogen bonded with the coordinated water molecules resulting in the formation of 1D linear chain (see Fig 8, top) instead of a zigzag chain in **2**. This difference in chain structure in **2** and **4** could be due to the aliphatic chain structure in the carboxylates; it is further evident from the orientation of t-butyl group in the bpta ligand with respect to the uncoordinated oxygen atom (O4) of the carboxylate group attached to the Ni(II) center - on the same side in **2** while on the opposite side in **4**. The presence of three lattice water molecules, which are further hydrogen bonded to coordinated water molecules and uncoordinated oxygen atoms of succinate, forms a 2D supramolecular assembly (Fig 8, bottom). Because of these hydrogen bonding interactions, four different motifs are formed. Motif 1 is $R_3^5(11)$ comprised of uncoordinated O atom of succinate (O5), carbon atoms of succinate, coordinated

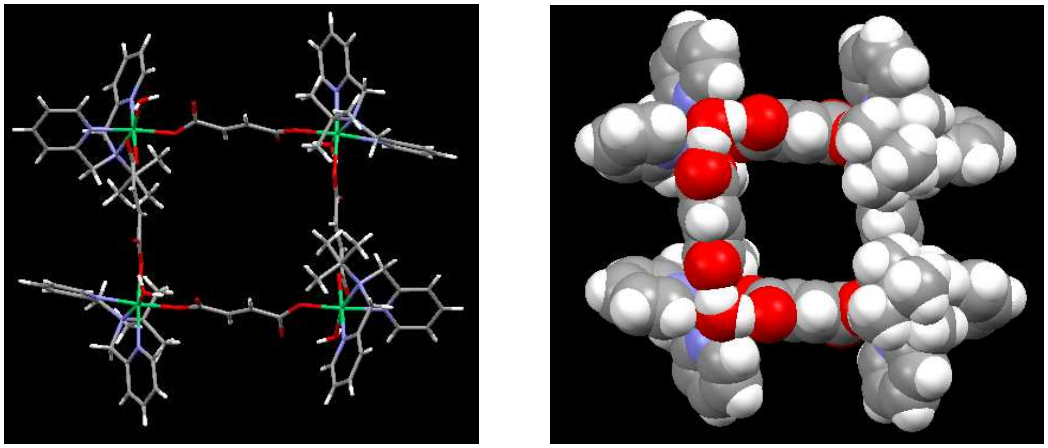

Fig. 5 A perspective view of **3** (left) and its space-fill model (right).

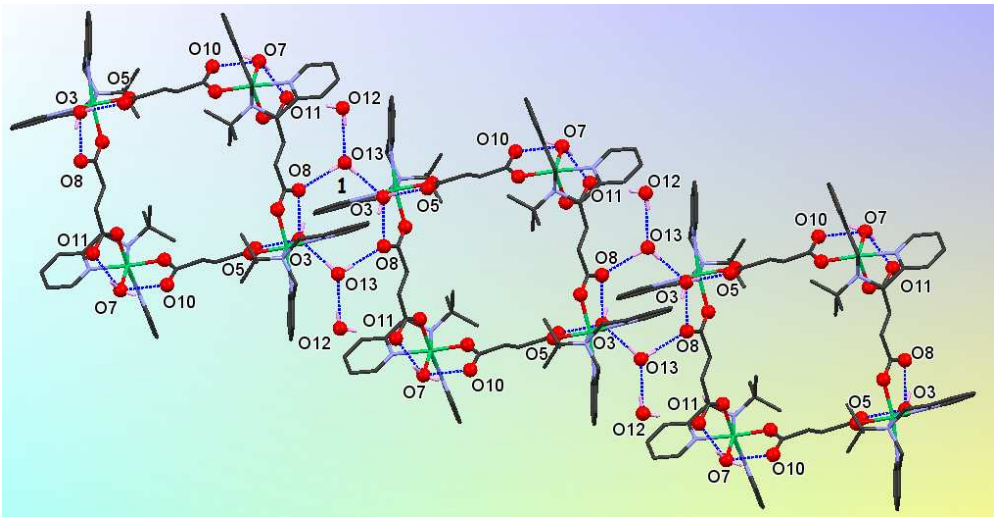

Fig. 6 Supramolecular assembly of squares in **3** showing a hexameric motif with two dangling monomers of water molecules.

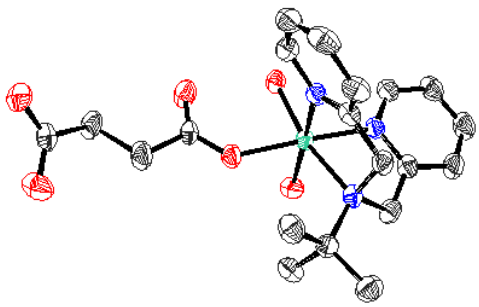

Fig. 7 An ORTEP view of **4**.

water molecule (O1) and the lattice water molecules (O7, O8 and O9). Motif 2 is $R_3^4(4)$ comprised of two lattice water molecules O8 and O9), coordinated water molecule (O2) on Ni(II) and uncoordinated oxygen atom of succinate (O6), Motif 3 is $R_5^8(12)$ comprised of comprised of three lattice water molecules (O7, O8 and O9), coordinated water molecules (O2 and O1) and succinate, and Motif 4 is $R_2^4(6)$ comprised of one carboxylate end (CO_2^-) of dicarboxylate (O5 and O6) and Ni (II) center with coordinated water molecules (O1 and O2). Four motifs in **4** vs three motifs in **2** could be responsible for the difference in their thermal properties (see the 'Thermogravimetric Analysis' section below). All the hydrogen bonding parameters are listed in Table 2.

None of the components in **4** is chiral in nature. Chirality in it is due to the orientation of the succinate linker. The succinate linker can have three rotamers - eclipsed, anti and gauche.[16-17] The gauche form is chiral and can form chiral compound from achiral components.[18-19] In **4**, its single crystal structure shows helical arrangement of the 1D chains in the supramolecular assembly formed through the hydrogen bonding interactions. Two adjacent right handed helices in **4** shown in Fig. S5 (ESI) possess a pitch height of 9.68 Å.

Journal Name RSCPublishing

ARTICLE

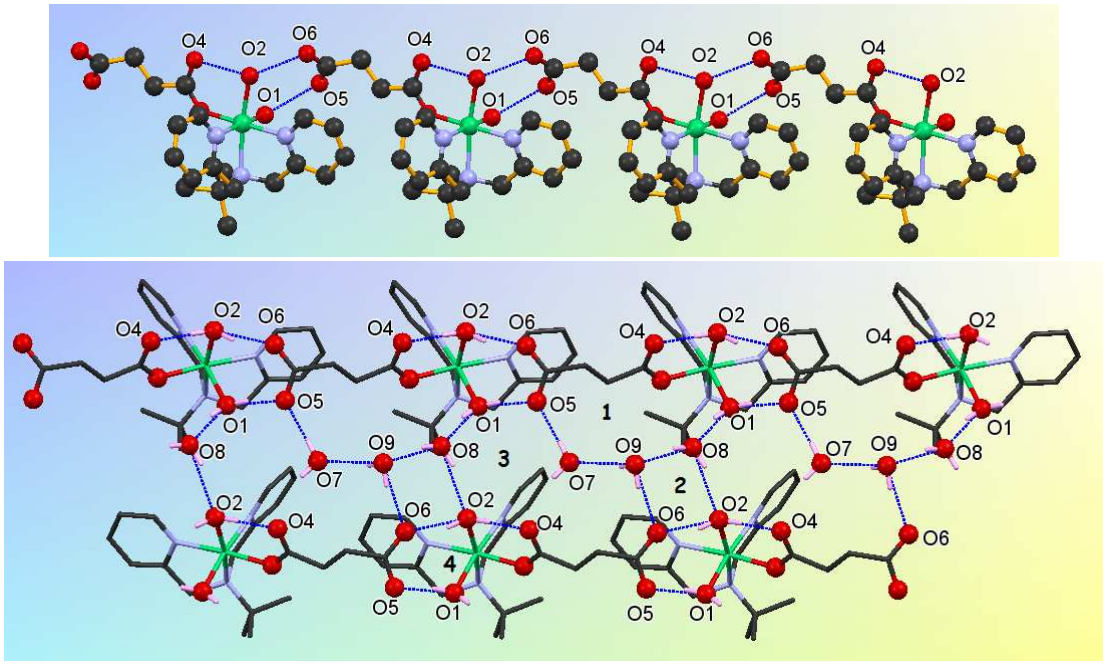

Fig. 8 1D linear chain of **4** (top) and hydrogen bonded network showing motifs in **4** (bottom); hanging contacts and hydrogens are deleted for clarity.

Role of Dicarboxylate Linkers. In this study, the dicarboxylate linkers with a triple bond (adc) to double bond (fumarate) to single bond (succinate) in the aliphatic chain structure between the carboxylate groups have been used to show any effect on the stability and properties of such supramolecular assemblies, particularly the structural diversity, of products in the Ni(II)-bpta system under similar reaction conditions. In case of adc this chain is linear and thus the carboxylate groups oriented in a linear fashion. On the other hand, for fumarate two carboxylate groups which are trans to each other with respect to the aliphatic chain structure bind in a syn-syn as well as syn-anti fashions in **3** (syn-anti is also observed elsewhere[16]). Thus the inherent rigidity in adc and fumarate could direct their binding to the metal centers. With a single bond between the two CH_2 groups in succinate, the orientation of the carboxylate groups directs to have the gauche form resulting chirality in **4**. As indicated above, the formation of **2**-**4** can be considered through the reaction of **1** with the respective dicarboxylic acid. Based on the final product formation, it is clear that the reaction of **1** with fumaric acid goes through a different pathway compared to the other two acids. This is described in Scheme 3. Although it is well observed for a polycarboxylic acid under hydrothermal condition not losing all protons for the charge balance, this is not the case for **2**-**4** which are made under non-hydrothermal conditions. This approach has made sure that both carboxylic acid groups get deprotonated forming the acetic acid by-product which is removed from the reaction pot by adding a mixture of acetonitrile-toluene followed by vacuum stripping of solvents. In **2** and **4**, only one carboxylate group (from adc and succinate, respectively) binds to each Ni(II) center and thus the remaining two coordination sites are occupied by two water molecules. On the other hand, in **3** there are two carboxylate groups from two different fumarate anions coordinated to each Ni(II) center leaving only one site available for the water molecule. In all cases, the N_{alkyl} atom of the bpta ligand is trans to the water molecule. Therefore, it is the binding difference of the carboxylate linker to the Ni(II)-bpta center that determines the number of coordinated water molecules on each Ni(II) ion. As mentioned earlier, the hydrogen bonding of these coordinated water molecules with the uncoordinated carboxylate groups of adc and succinate in **2** and **4**, respectively, is responsible for the formation of the supramolecular architectures in these. Thus the formation of **2**-**4** is primarily dependent on the skeletal difference of the dicarboxylates as the acidity of fumaric acid is in between those of acetylene dicarboxylic acid and succinic acid. The role of the dicarboxylates in determining the structure of such MOCNs is clearly demonstrated in this study.

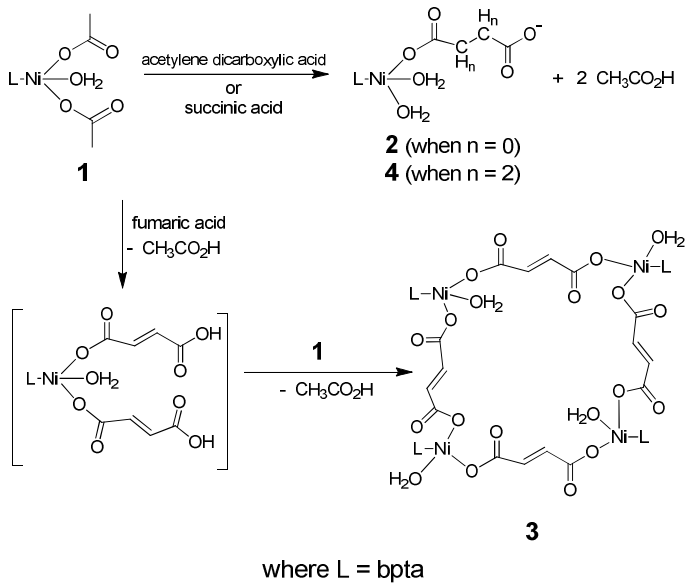

Scheme 3. A closer look into the formation of **2**, **3** and **4**.

FT-IR and Raman spectroscopy. The IR spectra of all the compounds were recorded in the solid state as KBr pellets. For **1** and **2** there are two broad peaks centered at 3516 and 3453 cm^{-1}; 3380 and 3233 cm^{-1} whereas for **3** and **4** there is one peak at 3402 and 3406 cm^{-1}, respectively, due to the O-H stretching frequency of water molecules present in these. It is important to note that in **2** the two bands are clearly separated but in **3** and **4** the second band is not seen indicating there is some difference in environment for two different water molecules (coordinated and lattice) in these assemblies as can be seen from their solid state structures. The carboxylates show asymmetric and symmetric stretching frequencies at 1640 and 1418 cm^{-1} (**1**), 1591 and 1343 cm^{-1} (**2**), 1567 and 1375 cm^{-1} (**3**), and 1565 and 1405 cm^{-1} (**4**), respectively. The different values of the carboxylate stretch for these three complexes suggest a different binding mode of the carboxylates as found in their crystal structures (*vide supra*). The peaks at 1607, 768, 676 cm^{-1} are due to the tridentate ligand and are common in all the compounds with a shift by few wave numbers. These were also studied by Raman spectroscopy. The peak at 2200 cm^{-1} corresponds to the C-C triple bond in **2** which is absent in **3** and **4** (see Figure S6, ESI).

Thermogravimetric Analysis. In order to understand the thermal stability and its structural variation as a function of temperature, thermogravimetric analysis (TGA) was carried out between 25-500 °C for all three compounds. All TGA scans are shown in Fig 9. The TGA scan of **1** is a three step profile. The first weight loss of 2.59% between 50-75 °C corresponds to loss of two-third of a lattice water molecule (ca. 2.56%). Due to the strong hydrogen bonding in **1** described above, the complete loss of lattice water did not occur at this temperature range. The second loss of 37.18% between 125-300 °C corresponds to the loss of the rest of lattice water molecule, one coordinated water molecule and two acetic acid molecule followed by continuous decomposition of the molecule. From the TGA scans it is clear that **3** is more stable than **2** and **4** which is also evident from the structural differences in their single crystal structures. The TGA scan of **2** is a three step profile. The first weight loss of 10.13% between 50-150 °C corresponds to loss of two lattice water molecules and one coordinated water molecules (ca. 10.84%). The second loss of 20.51% between 175-270 °C corresponds to the loss of one coordinated water molecule and acetylene dicarboxylic acid molecule followed by continuous decomposition of the molecule. The TGA scan of **3** is a two-step profile. The first weight loss of 3.88% between 150-175 °C corresponds to loss of four lattice water molecules (ca. 3.85%). After the loss of lattice water molecules the compound was stable up to ca. 300 °C followed by decomposition due to loss of fumaric acid. This shows its unusual stability. The TGA scan of **4** is a two-step profile. The first loss of 7.54% corresponds to the loss of two lattice water molecules (ca. 6.92%). This partial loss of lattice water molecules is similar to that observed for **2**. Further weight loss pattern of **4** is different from that of **2** and corresponds to the loss of one lattice water molecule and two coordinated water molecules and succinic acid.

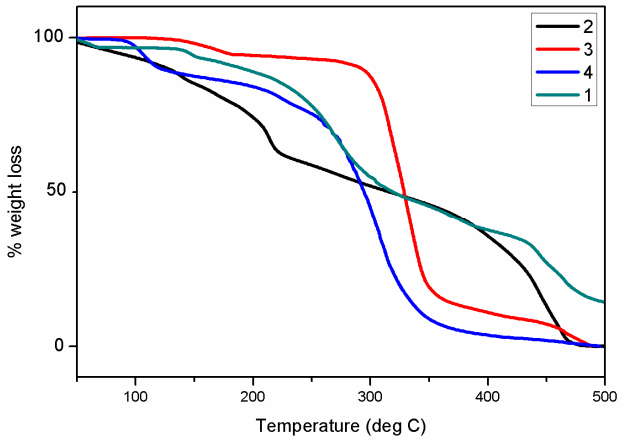

Fig. 9 TGA scans of **1**-**4**.

Experimental section

Materials and methods. All chemicals and solvents used for synthesis were obtained from commercial sources and were used as received, without further purification. All reactions were carried out under aerobic conditions. The bpta ligand was prepared by modifying the literature procedure.[20]

Physical measurements. The ^{1}H NMR spectrum of the ligand was obtained in $CDCl_3$ solution at 25°C on a BrukerARX-400 spectrometer; chemical shifts are reported relative to the residual solvent signals. The elemental analysis (C, H, N) was carried out using a Mettler CHNS analyzer, thermogravimetric analysis was carried out from 25 to 500 °C (at a heating rate of 10 °C/min) under dinitrogen atmosphere on a Mettler 851 E. IR spectra were measured in the 4000-400 cm^{-1} range on a Perkin-Elmer Spectrum I spectrometer with samples prepared as KBr pellets. Raman spectra were recorded on a Renishaw InVia Raman microscope equipped with a 785 nm high-power near-infrared laser working at 300 mW power and a Renishaw CCD detector. Analysis of the Raman spectra

were performed in reflection mode on powder samples placed on the sample stage and aligned in optical path by using a camera, with 10-50% laser power and by using 20-50x optics in the range of 500-4000 cm^{-1}.

$[Ni(bpta)(CH_3COO)_2(H_2O)]\cdot H_2O$ (**1**). 31.25 mg (0.125 mmol) of $Ni(OAc)_2$ and 32 mg (0.125mmol) of bpta were dissolved in 2 mL methanol. The reaction mixture was stirred for 3 hours at room temperature (RT) and evaporated to dryness under vacuum to isolate the product. Yield: 41 mg (70%). Single crystals were grown by slow evaporation of its methanolic solution. Anal. Calcd for $C_{20}H_{31}N_3NiO_6$ (MW 468.2): C, 51.28; H, 6.62; N, 8.71. Found: C, 50.93; H, 6.32; N, 9.02. Selected FTIR peaks (KBr, cm^{-1}): 3516, 3406, 1640, 1607, 1576 1484, 1418, 768, 755, 418.

$[Ni(bpta)(adc)(H_2O)_2]\cdot 2H_2O$ (**2**). 31.25 mg (0.125 mmol) of $Ni(OAc)_2$ and 32 mg (0.125mmol) of bpta were dissolved in 2 mL methanol. To this was added 14 mg (0.125 mmol) of acetylene dicarboxylic acid followed by the addition of 1 mL methanol. The reaction mixture was stirred for another 3 hours at RT, evaporated to dryness, treated with 2 mL acetonitrile-toluene mixture (1:1 v/v) and vacuum dried. Yield: 53 mg (81%). Single crystals were grown by cooling of its methanolic solution. Anal. Calcd for $C_{20}H_{29}N_3NiO_8$ (MW 498.2): C, 39.980; H, 3.718; N, 8.479. Found: C, 39.852; H, 3.658; N, 8.652.Selected FTIR peaks (KBr, cm^{-1}): 3384, 3233, 2975, 1605, 1591, 1343, 1026, 777, 767, 676. Selected Raman peaks (cm^{-1}): 2208,1610, 1570, 1373, 1229, 1029, 831, 614.

$[Ni_4(bpta)_4(fumarate)_4(H_2O)_4]\cdot 4H_2O$ (**3**). It was prepared following the procedure described above for **2** except 14.5 mg (0.125 mmol) of fumaric acid was used instead of acetylene dicarboxylic acid. Unlike **2**, a precipitate that appeared after 3 hours at RT was evaporated to dryness, treated with 2 mL acetonitrile-toluene mixture (1:1 v/v), and vacuum dried. A blue solid was obtained. Yield: 46 mg (80%). Single crystals were grown by slow evaporation of its aqueous solution. Anal. Calcd for $C_{80}H_{104}N_{12}Ni_4O_{23}$ (MW 1820.2): C, 52.22; H, 5.76; N, 9.14. Found: C, 52.23; H, 5.70; N, 8.66. It should be noted that the formula used for CHN analysis was with three water moleucle although other charcaterization techniques including X-ray crystallography indicated it had four water molecules. Selected FTIR peaks (KBr, cm^{-1}): 3402, 3024, 2967, 2918 1607, 1578, 1567, 1490, 1434, 1375, 1189, 1023, 987, 774, 764, 670, 652. Selected Raman peaks (cm^{-1}): 1654, 1608, 1571, 1574, 1449, 1403, 1260, 832, 644.

$[Ni(bpta)(succinate)(H_2O)_2]\cdot 3H_2O$ (**4**). It was prepared following the procedure described above for **1** except 15 mg (0.125 mmol) of succinic acid was used instead of dicarboxylic acid. Yield: 41 mg (56%). Single crystals were grown by slow evaporation of its methanolic solution. Anal. Calcd for $C_{20}H_{31}N_3NiO_7$ (MW 502.2): C, 49.79; H, 6.43; N, 8.71. Found: C, 49.84; H, 6.37; N, 8.83. It should be noted that the formula used for CHN analysis was with two water moleucles although other charcaterization techniques including X-ray crystallography indicated it had three water molecules. Selected FTIR peaks (KBr, cm^{-1}): 3406, 1608, 1565, 1487, 1254, 1024, 769, 659. Selected Raman peaks (cm^{-1}): 1610, 1575, 1451, 1228, 1028, 853, 831, 710, 645.

Single Crystal X-ray Structure Analysis. From a batch of crystals of each compound that was transferred from mother liquor to mineral oil for manipulation and selection, a single crystal was placed inside a nylon loop on a goniometer head followed by its slow cooling to the desired temperature under a cold stream of nitrogen gas provided by the LT device attached to the instrument. Initial crystal evaluation and data collection were performed on a Kappa APEX II diffractometer equipped with a CCD detector (with the crystal-to-detector distance fixed at 60 mm) and sealed-tube monochromated MoKα radiation and interfaced to a PC that controlled the crystal centering, unit cell determination, refinement of the cell parameters and data collection through the program APEX2.[21] By using the program SAINT[21] for the integration of the data, reflection profiles were fitted, and values of F^2 and $\sigma(F^2)$ for each reflection were obtained. Data were also corrected for Lorentz and polarization effects. The subroutine XPREP[21] was used for the processing of data that included determination of space group, application of an absorption correction (SADABS),[21] merging of data, and generation of files necessary for solution and refinement. The crystal structures were solved and refined using SHELX 97.[22] In each case, the space group was chosen based on systematic absences and confirmed by the successful refinement of the structure. Positions of most of the non-hydrogen atoms were obtained from a direct methods solution. Several full-matrix least-squares/difference Fourier cycles were performed, locating the remainder of the non-hydrogen atoms. In the final difference Fourier map in each case there was no other significant peaks >1 e/Å^3. All non-hydrogen atoms were refined with anisotropic displacement parameters. All hydrogen atoms of **1**-**4** except those for two coordinated water molecules in **2** and all water molecules in **4** were placed in ideal positions and refined as riding atoms with individual isotropic displacement parameters. Crystallographic parameters and basic information pertaining to data collection and structure refinement for all compounds are summarized in Table 1. All figures were drawn using ORTEP[23] and MERCURY V 3.0[24] and hydrogen bonding parameters were generated using PLATON.[25] The final positional and thermal parameters of the non-hydrogen atoms for all structures are listed in the CIF files (ESI).

Concluding Remarks

A variation in the dicarboxylates afforded diverse MOCNs under the same reaction conditions: the fumarate analogue $[Ni_4(bpta)_4(fumarate)_4(H_2O)_4]\cdot 4H_2O$ (**3**) is a square while the adc and succinate analogs $[Ni(bpta)(adc)(H_2O)_2]\cdot 2H_2O$ (**2**) and $[Ni(bpta)(succinate)(H_2O)_2]\cdot 3H_2O$ (**4**) are rare examples of Ni(II) monomeric subunit with only one end of the dicarboxylate coordinated. With the isolation and structural characterization of the intermediate for all, $[Ni(bpta)(OAc)_2(H_2O)]\cdot H_2O$ (**1**), it is clear that these carboxylates play an important role in determining the coordination architectures with respect to their size, conformation and properties. In addition to the variation in the dicarboxylates, the role of coordinated and lattice water molecules in the formation of these diverse MOCNs is also observed. This is highly correlated to their thermal behavior in the solid state. The current work has thus laid the foundation for

the strategy in developing new MOCNs with targeted structures and properties. It is envisaged that further chemical modifications on the N-donor ligand as well as choosing other metal centers will allow us to generate a series of MOCNs to understand their formation in detail.

Acknowledgements

Funding for this work was provided by IISER, Mohali. S. K. and V. G. are to grateful to CSIR and MHRD, India, respectively, for research fellowships. X-ray, NMR and Raman facilities at IISER, Mohali, and CIL, NIPER, Mohali for CHN analysis are gratefully acknowledged.

Notes

[a] Department of Chemical Sciences, Indian Institute of Science Education and Research, Mohali, Sector 81, Manauli PO, S.A.S. Nagar, Mohali (Punjab) 140306, INDIA
*e-mail: sanjaymandal@iisermohali.ac.in

† Footnotes should appear here. These might include comments relevant to but not central to the matter under discussion, limited experimental and spectral data, and crystallographic data.

Electronic Supplementary Information (ESI) available: crystallographic data of the structures **1-4** in CIF format (CCDC 979224 and 965620-22, respectively), additional figures for the crystal structures of **1**, **2** and **4** (Figs. S1-S5), Raman spectra for **2-4** (Fig. S6), and selected bond distances and angles of **1-4** (Table S1). See DOI: 10.1039/b000000x/

References

1. (a) J-M. Lehn, *Supramolecular Chemistry: Concepts and Perspectives*. VCH: New York, 1995. (b) J. W. Steed, J. L. Atwood, *Supramolecular Chemistry*. John Wiley & Sons, Ltd., 2009.
2. A. Dmitriev, N. Lin, J. V. Barth, K. Kern, *Angew. Chem. Int. Ed*., 2003, **42**, 2670.
3. (a) S. Kitagawa, R. Kitaura, S. Noro, *Angew. Chem. Int. Ed.,* 2004, **43**, 2334-2375; (b) D. J. Tranchemontagne, J. L. Mendoza-Cortés, M. O'Keeffe, O. M. Yaghi, *Chem. Soc. Rev.,*2009, **38**, 1257; (c) M. Kurmoo, *Chem. Soc. Rev*., 2009, **38**, 1353; (c) M. O'Keeffe, O. M. Yaghi, *Chem. Rev.,* 2012, **112**, 675; (d) M. K. Suh, H. J. Park, T. K. Prasad, D-W. Lim, *Chem. Rev.,* 2012, **112**, 782; (e) J-R. Li, J. Sculley, H-C. Zhou, *Chem. Rev.,* 2012, **112**, 869; (f) L. F. Kreno, K. Leong, O. K. Farha, M. Allendorf, R. P. Van Duyne, J. T. Hupp, *Chem. Rev.,* 2012, **112**, 1105; (g) Y. Cui, Y. Yue, G. Qian, G. Chen, *Chem. Rev.,* 2012, **112**, 1126.
4. (a) G. R. Desiraju, *Crystal Design: Structure and Functions (Perspectives in Supramolecular Chemistry)*. John Wiley & sons: England, 2003. (b) G. R. Desiraju, J. J. Vittal, A. Ramanan, *Crystal Engineering. A Text Book.* World Scientific Publishing Company: Singapore, 2011.
5. T. R. Cook, Y-R. Zheng, P. J. Stang, *Chem. Rev.,* 2013, **133**, 734.
6. N. Stock, S. Biswas, *Chem. Rev*., 2012, **112**, 933.
7. (a) C. G. Efthymiou, C. P. Raptopoulou, A. Terzis, R. Boča, M. Korabic, J. Mrozinski, S. P. Perlepes, E. G. Bakalbassis, *Eur. J. Inorg. Chem.* 2006, 2236; (b) R. Smith, D. Huskens, D. Daelemans, R. E. Mewis, C. D. Garcia, A. N. Cain, T. N. C. Freeman, C. Pannecouque, E. D. Clercq, D. Schols, T. J. Hubin, S. J. Archibald, *Chem. Phys. Lipids* 1990, **55**, 323.
8. (a) M. S. Bazarjani, S. Foro, W. Donner, A. Gurlo, R. Riedel, *Acta Crystallogr., Sect. E: Struct. Rep. Online*, 2012, **68**, m567; (b) T. C. Downie, W. Harrison, E. S. Raper, M. A. Hepworth, *Acta Crystallogr., Sect. B*, 1971, **27**, 706; (c) Werner, M.; Berner, J.; Jones, P. G., *Acta Crystallogr., Sect. C: Cryst. Struct. Commun.*, 1996, **52**, 72; (d) P. A. Williams, A. C. Jones, J. F. Bickley, A. Steiner, H. O. Davies, T. J. Leedham, S. A. Impey, J. Garcia, S. Allen, A. Rougier, A. Blyr, *J. Mater. Chem.* 2001, **11**, 2329.
9. J. P. Wikstrom, A. S. Filatov, E. A. Mikhalyova, M. Shatruk, B. Foxmane, E. V. Rybak-Akimova, *Dalton Trans.,* 2010, **39**, 2504.
10. S. Khullar, S. K. Mandal, *Cryst. Growth Des.,* 2012, **12**, 5329.
11. J. Kühnert, T. Rüffer, P. Ecorchard, B. Bräuer, Y. Lan, A. K. Powell, H. Lang, *Dalton Trans.,* 2009, 4499.
12. (a) R. Ludwig, *Angew. Chem. Int. Ed.,* 2001, **40**, 1808; (b) S. K. Ghosh, P. Bharadwaj, *Angew. Chem. Int. Ed.,* 2004, **43**, 3577.
13. (a) R. J. Saykally, D. J. Wales, *Science,* 2012*,* **336***,* 814; (b) K. Liu, J. D. Cruzan, R. J. Saykally, *Science,* 1996*,* **271***,* 929, and references therein.
14. H. Arora, F. Lloret, R. Mukherjee, *Dalton Trans.,* 2009, 9759.
15. M. D. Ward, A. Stephenson, *Dalton Trans.,* 2011, **40**, 10360.
16. S. Das, S. Maloth, S. Pal, *Eur. J. Inorg. Chem.,* 2011, 4270.
17. J. Zhang, Y. Kang, R-B. Zhang, Z-J. Li, J-K. Cheng, Y-G. Yao, *CrystEngComm,* 2005, **28**, 177.
18. K. Biradha, C. Seward, M. J. Zaworotko, *Angew. Chem. Int. Ed.,* 1999, **38**, 492.
19. T. Ezuhara, K. Endo, Y. Aoyama, *J. Am. Chem. Soc.,* 1999, **121***,* 3279.
20. H. J. Mok, J. A. Davis, S. Pal, S. K. Mandal, W. H. Armstrong, *Inorg. Chim. Acta,* 1997, **263**, 385.
21. *APEX2*, *SADABS and SAINT*; Bruker AXS inc: Madison, WI, USA, 2008.
22. G. M. Sheldrick, *Acta Crystallogr., Sect. A: Found. Crystallogr.*, 2008*,* **64***,* 112.
23. L. J. Farrugia, *Appl. Cryst.,* 1997, **30**, 565.
24. C. F. Macrae, I. J. Bruno, J. A. Chisholm, P. R. Edginton, P. McCabe, E. Pidocck, L. Rodriguez-Monge, T. Taylor, J. Van de Streek, P. A. Wood, *J. Appl. Crystallogr.,* 2008, **41**, 266.
25. A. L. Spek, PLATON, Version 1.62, University of Utrecht, 1999.

Table of contents – artwork and abstract

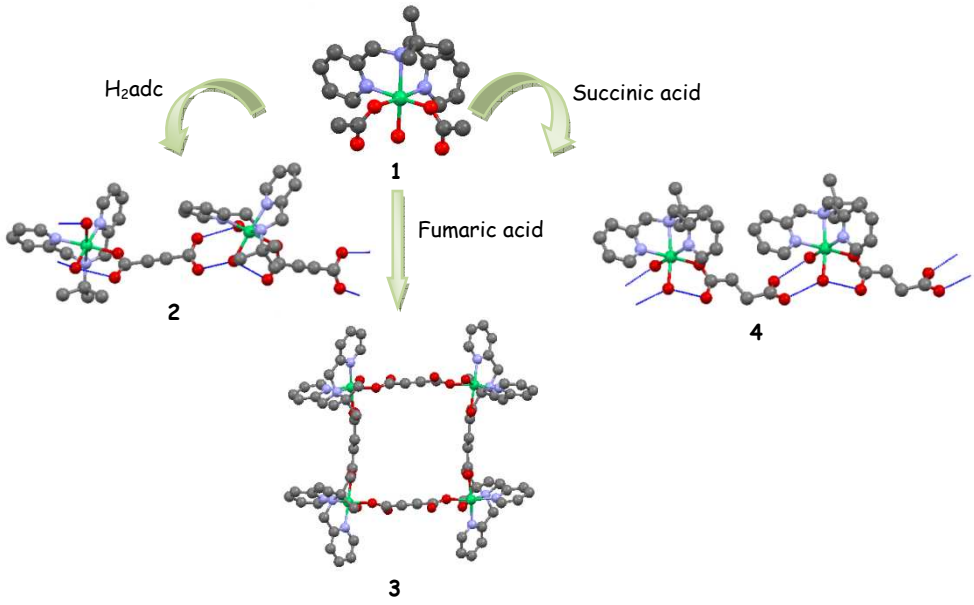

With a variation in the dicarboxylate linkers, diverse metal organic coordination networks generated under the same reaction conditions are reported: the fumarate analogue $[Ni_4(bpta)_4(fumarate)_4(H_2O)_4]\cdot 4H_2O$ (**3**) is a square while the adc and succinate analogs $[Ni(bpta)(adc)(H_2O)_2]\cdot 2H_2O$ (**2**) and $[Ni(bpta)(succinate)(H_2O)_2]\cdot 3H_2O$ (**4**) form 1D chains; further association of these through extensive hydrogen bonding network of lattice water, coordinated water and uncoordinated oxygen atoms of the carboxylate groups generate supramolecular assemblies of higher dimensions.